12

NASA CR 54244

BATT-4673-T2

DSR 5169-1

INVESTIGATION OF STABILITY PREDICTIONS OF FLUID-JET AMPLIFIER SYSTEMS

by

F. T. Brown, S. D. Graber and R. E. Wallhagen

Prepared for

NATIONAL AERONAUTICS AND SPACE ADMINISTRATION

Contract NAS 3-5203

ENGINEERING PROJECTS LABORATORY
MASSACHUSETTS INSTITUTE OF TECHNOLOGY

NOTICE

This report was prepared as an account of Government sponsored work. Neither the United States, nor the National Aeronautics and Space Administration (NASA), nor any person acting on behalf of NASA:

A.) Makes any warranty or representation, expressed or implied, with respect to the accuracy, completeness, or usefulness of the information contained in this report, or that the use of any information, apparatus, method, or process disclosed in this report may not infringe privately owned rights; or

B.) Assumes any liabilities with respect to the use of, or for damages resulting from the use of any information, apparatus, method or process disclosed in this report.

As used above, "person acting on behalf of NASA" includes any employee or contractor of NASA, or employee of such contractor, to the extent that such employee or contractor of NASA, or employee of such contractor prepares, disseminates, or provides access to, any information pursuant to his employment or contract with NASA, or his employment with such contractor.

Request for copies of this report should be referred to

National Aeronautics and Space Administration
Office of Scientific and Technical Information
Attention: AFSS-A
Washington, D.C. 20546

NASA CR 54244

DSR 5169-1

SEMI-ANNUAL REPORT

INVESTIGATION OF STABILITY PREDICTIONS OF FLUID-JET AMPLIFIER SYSTEMS

by

F. T. Brown, S. D. Graber and R. E. Wallhagen

Prepared for

NATIONAL AERONAUTICS AND SPACE ADMINISTRATION

October 30, 1964

Contract NAS 3-5203

Technical Management
NASA Lewis Research Center
Cleveland, Ohio
Advanced Development and Evaluation Division
William S. Griffin

ENGINEERING PROJECTS LABORATORY
MASSACHUSETTS INSTITUTE OF TECHNOLOGY
CAMBRIDGE, MASSACHUSETTS
02139

TABLE OF CONTENTS

ABSTRACT

1. INTRODUCTION 1

2. GENERAL STABILITY CRITERIA 3

   2.1. Low-Frequency Criterion 3

   2.2. High-Frequency Criterion 4

3. STABILITY OF AMPLIFIER DRIVING PISTON-CYLINDER LOAD 6

   3.1. Load With Negligible Connecting Lines 6

   3.2. Effect of Fluid Lines - Real Y_{11} and Y_{12} 9

   3.3. Effect of Fluid Lines - General Y_{11} and Y_{12} 15

4. EXPERIMENTAL APPARATUS AND TEST PROCEDURE-LOW FREQUENCY 18

5. EXPERIMENTAL RESULTS - HDL AMPLIFIER 26

6. HIGH FREQUENCY OR WAVE APPROACH 30

LIST OF FIGURES

1.	Piston-Cylinder Load	10
2.	Amplifier Driving Piston-Cylinder Load Through Significantly Long Lines	11
3.	Symmetric Piston-Cylinder Load with Lines	16
4.	Torque Motor, Flapper Valve, and Chamber of the Pneumatic Function Chamber	19
5.	Pneumatic Function Chamber	19
6.	HDL Proportional Amplifier Instrumented With Linear Flow Resistances and Pressure Transducers	20
7.	Instrumentation System	20
8.	Bridge Balance Circuit Diagram	22
9.	Schematic of Test Arrangement	23
10.	Light Beam Recorder Traces Giving First Two Columns of Eq. (42)	24
11.	HDL-Corning Single Stage Proportional Amplifier	27
12.	Corrected Resistance Relation of Mott Porous Disk	31
13.	Experimental Apparatus of L. E. Johnston	32
14.	Photographs of Johnston's Apparatus	33
15.	Measurements to Determine Reflection Coefficient	35

INVESTIGATION OF STABILITY PREDICTIONS OF FLUID-JET AMPLIFIER SYSTEMS

by

F. T. Brown, S. D. Graber and R. E. Wallhagen

17537 ABST

The first interim report under a contract with NASA describes the goal of a systematic approach toward the synthesis of fluid jet amplifiers and similar components into systems. The first step in the process is to measure the properties of the complex system components with adequate completeness. Two procedures are discussed: an admittance measuring approach which has been developed and operated, and a wave-scattering approach which is being planned. The second step is to use the component information to predict the dynamic response and stability. The emphasis herein is on stability; criteria are derived and applied to a few systems, two of which are checked experimentally. Finally, of course, one makes appropriate decisions, in the light of the predictions, regarding the system design.

Author →

1. INTRODUCTION

Systems involving fluid jet amplifiers and similar components are presently designed on an ad hoc and empirical basis, without adequate information about the components. The purpose of the present contract with NASA, which started last May and continues until next September, is to explore practical techniques for measuring the characteristics of the complex active elements in any given system, predicting directly the characteristics of the simpler passive elements, and finally putting all this information together to anticipate the over-all performance of the system. In this way it is hoped that design of such systems will become more streamlined and routine, that more optimum components and systems will be realized, and that a better understanding of the properties and processes will accrue.

The emphasis of the project and particularly this first interim report is the stability of systems. It is not uncommon to find wildly oscillatory instabilities in systems which are built from quite stable components. Also, much higher frequency "noise" frequently is suspected of being a camouflaged superposition of predicable instabilities that might be avoided if understood.

The larger question of dynamic response also is of interest, although thus far it has not been emphasized.

Fluid jet amplifiers and other "pure fluid" system components behave more or less nonlinearly. Nevertheless, like almost any other system, their behavior can be linearized for small excursions from some nominal state, as long as no discontinuities are locally involved. This linearization effects great simplifications in the dynamic analysis. Moreover, a system dynamically unstable "in the small" usually has very large limit cycles, and a system stable for small disturbances is usually also stable for large disturbances. Therefore, the analysis and experiment has been keyed to the linearization approach. Never-

theless, its limitations are fully recognized; the range of the linearized "coefficients" for different operating states is of particular importance.

Two approaches have been proposed. One, the admittance approach, is keyed to the easiest kind of experimental technique for measuring the characteristics of a component at zero and low frequencies. Basically, the pressures at all the n-ports except one of the multiport component being tested are held constant, and that one is oscillated. The flows at all the ports are then measured. Repeating the experiment with the variable pressure consecutively at each other port completes a matrix of n^2 admittances which completely describes the system at the test frequency and within the linearization assumption. This approach is being developed first, and occupies the bulk of this report. At high frequencies it becomes impractical, however.

The other approach, appropriate for quite high frequencies, involves acoustic testing of the components. The fundamental idea is observation and measurement of the reflected and refracted waves resulting from an incident wave. Sine waves appear the most practical, since easily measured standing and travelling wave patterns occur. The results of the measurements is a matrix of n^2 wave-scattering (reflection and refraction) coefficients.

Stability and dynamic response can be predicted using either the admittances or the wave-scattering coefficients. Derivations of the stability criteria are given in Sec. 2. In Secs. 3, 4, and 5 the low-frequency approach is illustrated in both its analytic and experimental aspects. Section 6 deals with the high-frequency approach, which presently is in the planning stage.

Projected plans for the duration of the contract include further development of the test procedures, collection of considerable test data for a few widely used amplifiers, and demonstration of the application and usefulness of the results.

2. GENERAL STABILITY CRITERIA

The two stability criteria, one expressed in terms of admittance matrices and useful for low-frequencies and the other expressed in terms of wave scattering matrices and useful for high frequencies, are given in a paper[+] by one of the authors. The material below is complementary to this paper, and includes missing derivations of the criteria.

2.1. Low-Frequency Criterion

The entire system under consideration is divided into two subsystems with n-ports of intercoupling. The small disturbance linearized characteristics then can be expressed in terms of two square admittance matrices, $\mathbf{Y}$ and $\mathbf{Y}'$, corresponding to the two subsystems. The diagonal elements of these matrices are termed the self-admittances, and the non-diagonal elements the transfer admittances.

$$\mathbf{w} = \mathbf{Y}(D)\,\mathbf{p} + \mathbf{w}_o \qquad (1)$$
$$\mathbf{w}' = \mathbf{Y}'(D)\,\mathbf{p} + \mathbf{w}_o'.$$

Here $\mathbf{w}$ and $\mathbf{w}'$ are column matrices representing the respective flows, which are positive when directed into the respective subsystems; $\mathbf{w}_o$ and $\mathbf{w}_o'$ are the flows when the pressures $\mathbf{p}$, which are shared commonly, are zero; $\mathbf{Y}$ and $\mathbf{Y}'$ are in general functions of $D \equiv d/dt$, the derivative operator (a result of the assumption of linear dynamics).

The derivative forms

$$d\mathbf{w} = \mathbf{Y}(D)\,d\mathbf{p} \qquad (2)$$
$$d\mathbf{w}' = \mathbf{Y}'(D)\,d\mathbf{p}$$

[+] Brown, F.T., "On the Stability of Fluid Systems", Proceedings of the Fluid Amplification Symposium, Harry Diamond Laboratories, Washington, D.C., Vol. 1, May 1964.

have a sum equal to zero, giving

$$\left[\mathbf{Y}(D) + \mathbf{Y}'(D)\right] \quad d\mathbf{p} = 0. \tag{3}$$

Particular solutions to this classical equation are of the form

$$d\mathbf{p} = s^{s_n t} \quad d\mathbf{p}_o, \tag{4}$$

giving

$$\left[\mathbf{Y}\ (s_n) + \mathbf{Y}'\ (s_n)\right] \quad d\mathbf{p}_o = 0; \tag{5}$$

for nontrivial solutions this requires

$$\det \left[\mathbf{Y}\ (s_n) + \mathbf{Y}'\ (s_n)\right] = 0. \tag{6}$$

The necessary and sufficient condition of stability is that all values of s_n have negative real parts, so that Eq. (4) does not show an infinitesimal disturbance building up to a nonlinearity-limited large disturbance; i. e., the zeroes of the determinant must all be in the left half of the s-plane. As pointed out in the above mentioned paper and numerous texts on control theory (usually under the heading "Nyquist criterion"), the existence of right-half plane zeroes is usually best determined by mapping the boundary of the right half of the s-plane into the complex plane of the determinant itself. The closed boundary of the s-plane gives a closed curve in the determinant plane; right half plane zeroes of the s-plane are revealed by net encirclements of the origin in the determinant plane. This procedure is illustrated in the paper and in Sec. 3 of this report.

2.2. High-Frequency Criterion

It is very difficult to directly measure the admittance matrix of an amplifier at very high frequencies. Thus an alternative wave-interaction approach is suggested, in which the same two subsystems are described by their square wave-scattering matrices $\mathbf{S}$ and $\mathbf{S}'$:

$$d\mathbf{v} = \mathbf{S}(D)\, d\mathbf{u}$$

$$d\mathbf{v}' = \mathbf{S}'(D)\, d\mathbf{u}'. \tag{7}$$

Here $d\mathbf{u}$ and $d\mathbf{u}'$ are infinitesimal waves incident at the n-ports of the respective subsystems, and $d\mathbf{v}$ and $d\mathbf{v}'$ are the resulting waves emanating from the n-ports. When the subsystems are joined together,

$$d\mathbf{u} = d\mathbf{v}'$$

$$d\mathbf{u}' = d\mathbf{v}, \tag{8}$$

so that

$$\left[\mathbf{\Pi} - \mathbf{S}'(D)\, \mathbf{S}\,(D)\right] \quad d\mathbf{u} = 0. \tag{9}$$

This result is analogous to Eq. (5); for stability, the determinant $\left|\mathbf{\Pi} - \mathbf{S}'\,(s_n)\, \mathbf{S}\,(s_n)\right|$ must have no zeroes in the right half plane, etc.

Applications of this result are also given in the before-mentioned paper. Plans for the current contract include its use; See Sec. 6.

3. STABILITY OF AMPLIFIER DRIVING PISTON-CYLINDER LOAD

Piston-cylinder loads are frequently used, and often give serious instabilities. First we will consider this load without the effects of long connecting lines, then with connecting lines. The work thus far is strictly analytical; experiments will be carried out later.

3.1. Load With Negligible Connecting Lines

The load is shown in Fig. 1, including the definitions of positive flows. Beneath the associated bond graph[+] the corresponding transmission matrix cascade is shown. The product of these three matrices is

$$\begin{bmatrix} p_1 \\ w_1 \end{bmatrix} = \begin{bmatrix} A & B \\ C & D \end{bmatrix} \begin{bmatrix} p_2 \\ -w_2 \end{bmatrix} \tag{10}$$

where

$$A \equiv 1 + IC_2D^2$$
$$B \equiv ID$$
$$C \equiv C_1D\,(1 + IC_2D^2) + C_2D$$
$$D \equiv 1 + IC_1D^2$$

The corresponding admittance matrix Y' is desired so that the stability criterion involving Eq. (6) can be employed:

$$\begin{bmatrix} w_1 \\ w_2 \end{bmatrix} = \begin{bmatrix} Y_{11}' & Y_{12}' \\ Y_{21}' & Y_{22}' \end{bmatrix} \begin{bmatrix} p_1 \\ p_2 \end{bmatrix} = \begin{bmatrix} \frac{D}{B} & -\frac{1}{B} \\ -\frac{1}{B} & \frac{A}{B} \end{bmatrix} \begin{bmatrix} p_1 \\ p_2 \end{bmatrix} \tag{11}$$

Here use has been made of the fact that

$$\Delta \equiv AD - BC = 1 \tag{12}$$

[+] The techniques employed are described in H. M. Paynter, "Analysis and Design of Engineering Systems", M.I.T. Press, 1960.

which is a requirement of passive linear systems.[++] The admittance matrix for the output ports of the amplifier is

$$\mathbf{Y} \equiv \begin{bmatrix} Y_{11} & Y_{12} \\ Y_{21} & Y_{22} \end{bmatrix} \tag{13}$$

so that the determinant of interest is

$$\left|\mathbf{Y} + \mathbf{Y}'\right| = \begin{bmatrix} Y_{11} + \dfrac{1 + IC_1 s^2}{Is} & Y_{12} - \dfrac{1}{Is} \\ Y_{21} - \dfrac{1}{Is} & Y_{22} + \dfrac{1 + IC_2 s^2}{Is} \end{bmatrix} \tag{14}$$

Here we will consider only the symmetrical case, for which

$$\begin{aligned} Y_{11} &= Y_{22} \\ Y_{12} &= Y_{21} \\ C_1 &= C_2 = C \end{aligned} \tag{15}$$

so that

$$\left|\mathbf{Y} + \mathbf{Y}'\right| = Y_{11}^2 - Y_{12}^2 + 2Y_{11}\,\frac{1 + IC\,s^2}{Is} + 2\,\frac{C}{I} + C^2 s^2 + 2\,\frac{Y_{12}}{Is} \tag{16}$$

Evaluating this for $s = j\omega$ gives

[++] This follows directly from the reciprocity theorem, which requires $Y_{12}' = Y_{21}'$.

$$\left|Y + Y'\right| = Y_{11}^2 - Y_{12}^2 + 2\frac{C}{I} - C^2\omega^2 - \frac{2j}{I\omega}\left[(1 - IC\omega^2)\,Y_{11} + Y_{12}\right] \quad (17)$$

The complex plane locus of this determinant is shown very crudely in Fig. 1; the locus is completed for $s = \infty$, so that the boundary of the entire right-half of the s-plane is mapped. For no net encirclements of the origin, the intercept of the locus with the real axis must be to the right of the origin.

For real Y_{11} and Y_{12} this intercept occurs when

$$(1 - IC\omega^2)\,Y_{11} + Y_{12} = 0$$

or

$$C^2\omega^2 = \frac{C}{I}\left(1 + \frac{Y_{12}}{Y_{11}}\right) \quad (18)$$

and the condition of stability for this special but important case becomes

$$Y_{11}^2 - Y_{12}^2 + \left(1 - \frac{Y_{12}}{Y_{11}}\right)\frac{C}{I} \geq 0$$

or

$$(Y_{11} - Y_{12})\left(Y_{11} + Y_{12} + \frac{1}{Y_{11}}\,\frac{C}{I}\right) \geq 0 \quad (19)$$

Normally,

$$Y_{11} > 0;\ Y_{12} < 0 \quad (20)$$

in which case the presence of the piston and the cylinder is a stabilizing influence. If the cylinder compliance is essentially zero, or the piston mass essentially infinite, the condition of stability is simply

$$\left|Y_{11}\right| > \left|Y_{12}\right| \tag{21}$$

These particular solutions have been checked by independent derivations.

3.2. Effect of Fluid Lines - Real Y_{11} and Y_{12}

The piston-cylinder load without damping is a conservative system. Therefore, any system instability can be associated with the amplifier itself. Specifically, in the system with lines connecting the amplifier and load (Fig. 2) an instability requires an energy amplification of waves, travelling in the lines incident on the amplifier. The energy in waves of equal shape is proportional to the square of their amplitude. The amplitudes of the reflected wave and the wave refracted into the other line are, respectively,

$$\begin{aligned} u_2 &= r_\ell v_2 \\ v_1 &= r_r v_2 \end{aligned} \tag{22}$$

where v_2 is the amplitude of the incident wave, r_ℓ is the reflection coefficient, and r_r is the refraction coefficient. Note the inherent assumption that Y_{12} and Y_{11} are real, which follows from the assumption of equal-shaped incident, reflected and refracted waves. The transmission matrix and admission matrix forms of the relationships between the pressure-flow variables are

$$\begin{bmatrix} p_1 \\ w_1 \end{bmatrix} = \begin{bmatrix} A & B \\ C & D \end{bmatrix} \begin{bmatrix} p_2 \\ -w_2 \end{bmatrix} \tag{23}$$

$$\begin{bmatrix} w_1 \\ -w_2 \end{bmatrix} = \begin{bmatrix} Y_{11} & Y_{12} \\ Y_{21} & -Y_{22} \end{bmatrix} \begin{bmatrix} p_1 \\ p_2 \end{bmatrix} = \begin{bmatrix} \frac{D}{B} & -\frac{\Delta}{B} \\ \frac{1}{B} & -\frac{A}{B} \end{bmatrix} \begin{bmatrix} p_1 \\ p_2 \end{bmatrix} \tag{24}$$

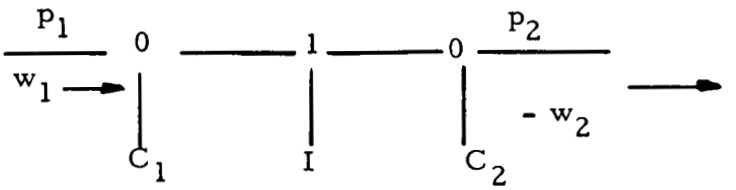

$$\begin{bmatrix} p_1 \\ w_1 \end{bmatrix} = \begin{bmatrix} 1 & 0 \\ C_1 D & 1 \end{bmatrix} \begin{bmatrix} 1 & ID \\ 0 & 1 \end{bmatrix} \begin{bmatrix} 1 & 0 \\ C_2 D & 1 \end{bmatrix} \begin{bmatrix} p_2 \\ -w_2 \end{bmatrix}$$

compliances: $C_1 = \dfrac{\rho V_1}{\beta}$; $C_2 = \dfrac{\rho V_2}{\beta}$

Effective inertia: $I = \dfrac{m}{\rho A^2}$

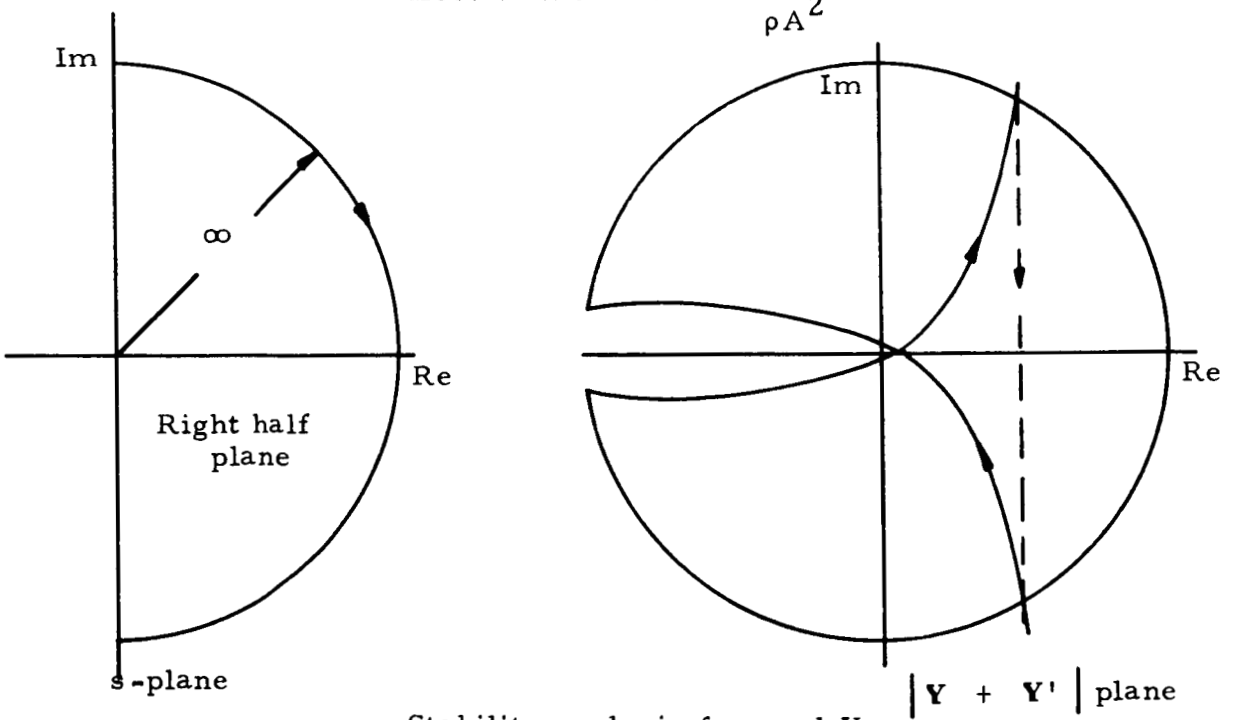

Stability analysis for real **Y**

Fig. 1. Piston-Cylinder Load.

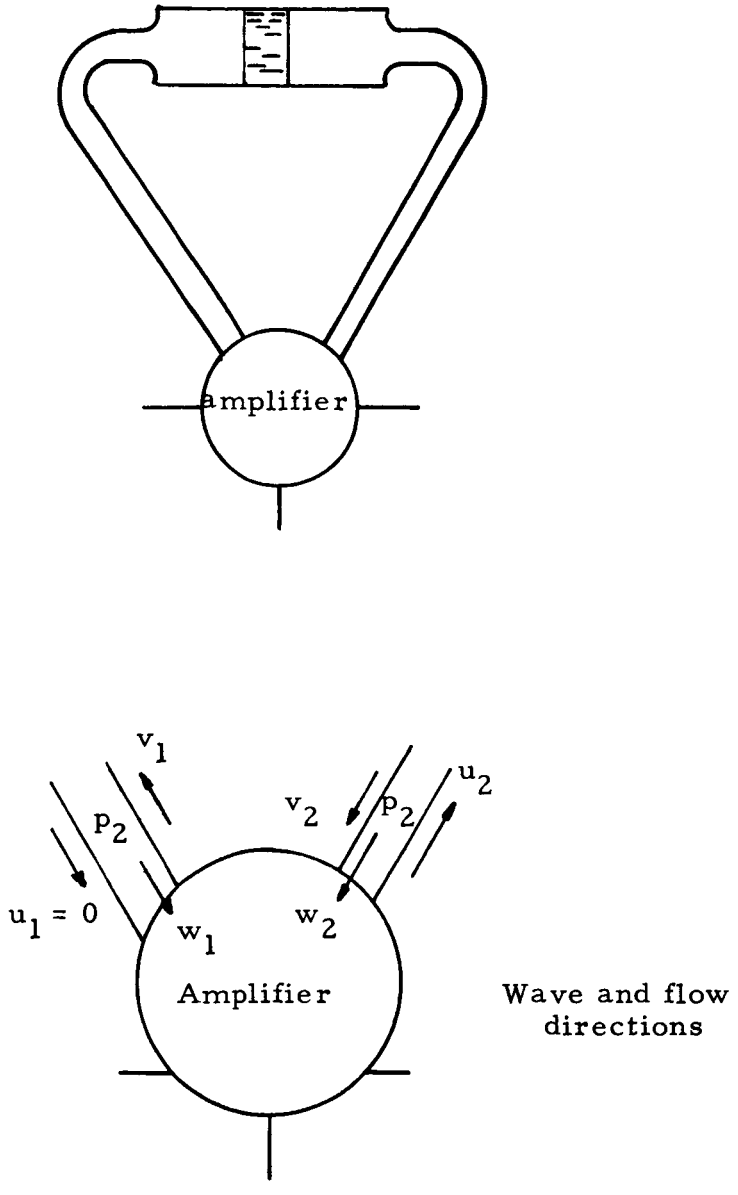

Fig. 2. Amplifier Driving Piston-Cylinder Load Through Significantly Long Lines.

So that, in the symmetric case ($Y_{11} = Y_{22}$; $Y_{21} = Y_{12}$; $\Delta \equiv AD - BC = 1$)

$$A = D = - \frac{Y_{11}}{Y_{12}}$$

$$B = - \frac{1}{Y_{12}} \tag{25}$$

$$C = - \frac{Y_{11}^2 - Y_{12}^2}{Y_{12}}$$

The relation between the waves is

$$\begin{bmatrix} u_1 \\ v_1 \end{bmatrix} = \frac{1}{\sqrt{2}} \begin{bmatrix} 1 & 1 \\ 1 & -1 \end{bmatrix} \begin{bmatrix} \frac{1}{\sqrt{Z_c}} & 0 \\ 0 & \sqrt{Z_c} \end{bmatrix} \begin{bmatrix} A & B \\ C & D \end{bmatrix} \begin{bmatrix} \sqrt{Z_c} & 0 \\ 0 & \frac{1}{\sqrt{Z_c}} \end{bmatrix} \frac{1}{\sqrt{2}} \begin{bmatrix} 1 & 1 \\ 1 & -1 \end{bmatrix} \begin{bmatrix} u_2 \\ v_2 \end{bmatrix}$$

$$= \frac{1}{2} \left[\begin{array}{cc|cc} A + \frac{B}{Z_c} + Z_c C + D & & A - \frac{B}{Z_c} + Z_c C - D & \\ & & & \\ A + \frac{B}{Z_c} - Z_c C - D & & A - \frac{B}{Z_c} - Z_c C + D & \end{array}\right] \begin{bmatrix} u_2 \\ v_2 \end{bmatrix}$$

$$\equiv \begin{bmatrix} s_{11} & s_{12} \\ s_{21} & s_{22} \end{bmatrix} \begin{bmatrix} u_2 \\ v_2 \end{bmatrix} = \mathbf{S} \begin{bmatrix} u_2 \\ v_2 \end{bmatrix} \tag{26}$$

where Z_c is the characteristic impedance of the lines, and **S** is the wave-scattering matrix. If u_1 is set equal to zero, the reflection and refraction coefficients are

$$r_\ell = - \frac{s_{12}}{s_{11}}$$

$$r_r = \frac{s_{11}\, s_{22} - s_{12}\, s_{21}}{- s_{11}} \tag{27}$$

which gives

$$r_\ell = \frac{1 - Z_c^{\,2} (Y_{11}^{\,2} - Y_{12}^{\,2})}{1 + Z_c^{\,2} (Y_{11}^{\,2} - Y_{12}^{\,2}) + 2Y_{11}\, Z_c}$$

$$r_r = \frac{- 2Z_c\, Y_{12}}{1 + Z_c^{\,2} (Y_{11}^{\,2} - Y_{12}^{\,2}) + 2Y_{11}\, Z_c} \tag{28}$$

The criterion of an active energy source is that the energy in the sum of the reflected and refracted waves is greater than in the incident wave. Thus if there is no energy dissipation in the rest of a system which contains the element in question, the criterion of stability is

$$r_\ell^{\,2} + r_r^{\,2} \leq 1 \tag{29}$$

which gives

$$(Y_{11}^{\,2} - Y_{12}^{\,2})\,(2 + Y_{11} Z_c) Z_c + Y_{11} \geq 0. \tag{30}$$

If Y_{11} is assumed to be positive, an essential sufficient (and almost necessary) condition is

$$\left|Y_{11}\right| > \left|Y_{12}\right| . \tag{31}$$

In the asymmetric case,

$$A = -\frac{Y_{22}}{Y_{21}} ; \quad D = -\frac{Y_{11}}{Y_{21}}$$

$$B = -\frac{1}{Y_{21}} \tag{32}$$

$$C = -\frac{Y_{11}\,Y_{22} - Y_{12}\,Y_{21}}{Y_{21}}$$

yielding

$$r_\ell = \frac{1 - Z_c^{\,2}\,(Y_{11}Y_{22} - Y_{12}\,Y_{21}) + Z_c(Y_{11} - Y_{22})}{1 + Z_c^{\,2}\,(Y_{11}Y_{22} - Y_{12}Y_{21}) + Z_c(Y_{11} + Y_{22})}$$

$$r_r = \frac{-2\,Z_c\,Y_{12}}{1 + Z_c^{\,2}\,(Y_{11}Y_{22} - Y_{12}Y_{21}) + Z_c(Y_{11} + Y_{22})} \tag{33}$$

and for stability,

$$Z_c(2Y_{11}Y_{22} - Y_{21}Y_{12} - Y_{12}^2) + Z_c^2 Y_{11}(Y_{11}Y_{22} - Y_{12}Y_{21}) + Y_{22} > 0 \tag{34}$$

It should be recognized that the results of Eqs. (33) and (34) above apply to waves incident on side number 2; for waves incident on side number 1, the subscripts 1 and 2 can be interchanged. Thus, two criteria of stability must be satisfied simultaneously, because waves can and will travel in both directions.

These results will be used in Sec. 5.

3.3. Effect of Fluid Lines - General Y_{11} and Y_{12}

When the elements of the admittance matrix Y are not real, that is when the dynamic behavior of the amplifier deviates significantly from the static behavior, it becomes necessary to consider the dynamics of the load also. In this section a symmetric piston-cylinder load connected with equal length lines to the output ports of a symmetric amplifier, as shown in Fig. 2, again will be investigated.

The load itself is shown in Fig. 3, with the corresponding bond graph and matrix cascade, which takes advantage of results found earlier. Consequently,

$$\begin{bmatrix} p_1 \\ w_1 \end{bmatrix} = \begin{bmatrix} A & B \\ C & D \end{bmatrix} \begin{bmatrix} p_2 \\ w_2 \end{bmatrix} \tag{35}$$

in which

$$A = D = p \cosh 2\Gamma + q \sinh 2\Gamma$$

$$B = Z_c \left[q \cosh 2\Gamma + p \sinh 2\Gamma - r \right] \tag{36}$$

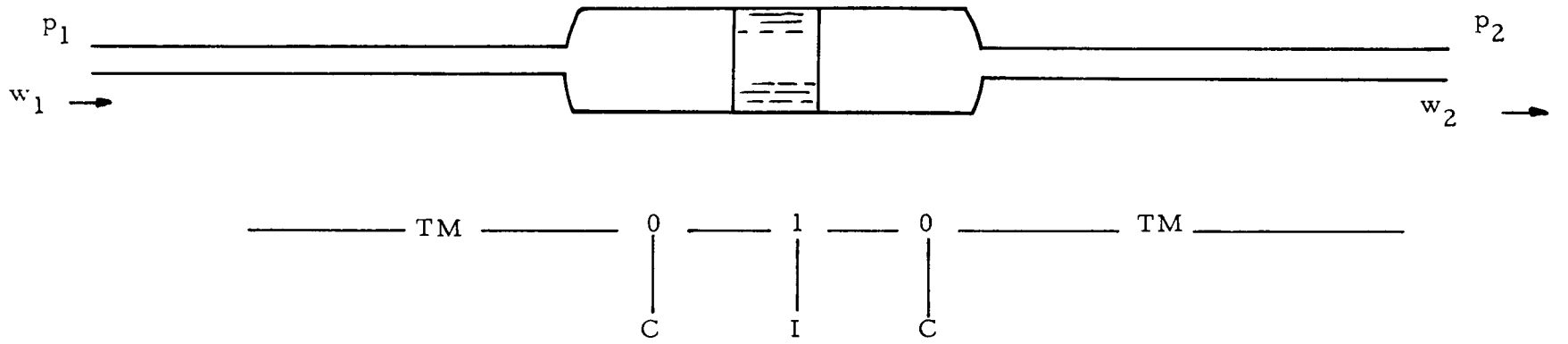

$$\begin{bmatrix} p_1 \\ w_1 \end{bmatrix} = \begin{bmatrix} \cosh \Gamma & Z_c \sinh \Gamma \\ \frac{1}{Z_c} \sinh \Gamma & \cosh \Gamma \end{bmatrix} \begin{bmatrix} 1 + ICD^2 & ID \\ CD(2 + ICD)^2 & 1 + ICD^2 \end{bmatrix} \begin{bmatrix} \cosh \Gamma & Z_c \sinh \Gamma \\ \frac{1}{Z_c} \sinh \Gamma & \cosh \Gamma \end{bmatrix} \begin{bmatrix} p_2 \\ w_2 \end{bmatrix}$$

Γ = TD, where T is the wave travel time for one line, one way.

Fig. 3. Symmetric Piston-Cylinder Load with Lines.

$$C = \frac{1}{Z_c} \left[q \cosh 2\Gamma + p \sinh 2\Gamma + r \right]$$

where

$$p \equiv 1 + ICD^2$$

$$q \equiv CDZ_c + \frac{IC^2D^3Z_c}{2} + \frac{ID}{2Z_c} \qquad (37)$$

$$r \equiv q - \frac{ID}{Z_c}$$

The equivalent admittance matrix is

$$\begin{bmatrix} w_1 \\ -w_2 \end{bmatrix} = \begin{bmatrix} Y_{11}' & Y_{12}' \\ Y_{21}' & Y_{22}' \end{bmatrix} \begin{bmatrix} p_1 \\ p_2 \end{bmatrix} = \begin{bmatrix} \frac{D}{B} & -\frac{1}{B} \\ -\frac{1}{B} & \frac{A}{B} \end{bmatrix} \begin{bmatrix} p_1 \\ p_2 \end{bmatrix} \qquad (38)$$

Thus the determinant used in the stability analysis becomes

$$\left| Y + Y' \right| = \begin{bmatrix} \frac{Y_{11} + \frac{A}{B}}{Y_{12} - \frac{1}{B}} & - \end{bmatrix} \left| \begin{matrix} \frac{Y_{12} - \frac{1}{B}}{Y_{11} + \frac{A}{B}} & - \end{matrix} \right| \qquad (39)$$

$$= Y_{11}^2 - Y_{12}^2 + 2 \frac{Y_{11}A + Y_{12}}{B} + \frac{A^2 - 1}{B^2} \qquad (40)$$

Equation (16) is actually a special case of this result. Further analysis should be based on the specific character of Y_{11} and Y_{12}, and would involve complex plane plots, etc.

4. EXPERIMENTAL APPARATUS AND TEST PROCEDURE-LOW FREQUENCY

The low frequency test apparatus consists basically of a pneumatic sine wave generator which causes a small periodic disturbance at one port of the element being tested, and the instrumentation system which measures the effect of the disturbance at the various ports.

The pneumatic sine wave generator, Fig. 4, is part of a system designed and built at M.I.T. by D. A. Korenstein.[+] A pressure wave is generated in a variable volume chamber which receives low pressure air flow and discharges part of it through an orifice restricted by a flapper. The flapper is driven sinusoidally by a proportional torque motor which is in turn driven by a low frequency electronic oscillator and servo amplifier (Fig. 5). A tube carries the signal from the chamber to a port of the amplifier being tested.

Figure 6 shows a Harry Diamond Laboratories and Corning Glass Works proportional amplifier instrumented for testing. The line entering from the left is from the wave generator. The remaining ports (not connected in the picture) are normally connected to constant-pressure sources. Such sources are obtained by putting a tee in the flow lines from the pressure regulators which brings each line into communication with an accumulator, filtering out pressure fluctuations. Standard air bottles are used for the accumulators. The control and exhaust port flows are measured by monitoring the pressure drops across linear flow resistances (Hoke air filters with element No. 2231[++]) placed in the lines. The pressure drops are indicated by strain gage differential pressure transducers (CEC $\pm$ 5 psid for control flow $\pm$ 15 psid for output flow). An additional pressure transducer measures the gage pressure upstream of the excited port. The other components of the instrumentation system are shown in Fig. 7. In the foreground are the power supply (5 - 10 V D-C) for the pressure transducers, the control unit, and a CEC light-beam recorder.

[+] Design of a Pneumatic Function Generator, Thesis (S.M.), EPL., M.I.T. August 1962.

[++] Spec. sheets 6-30 rev. 1/64 and 6-32, 2/63 Hoke Inc., Creshill, New Jersey.

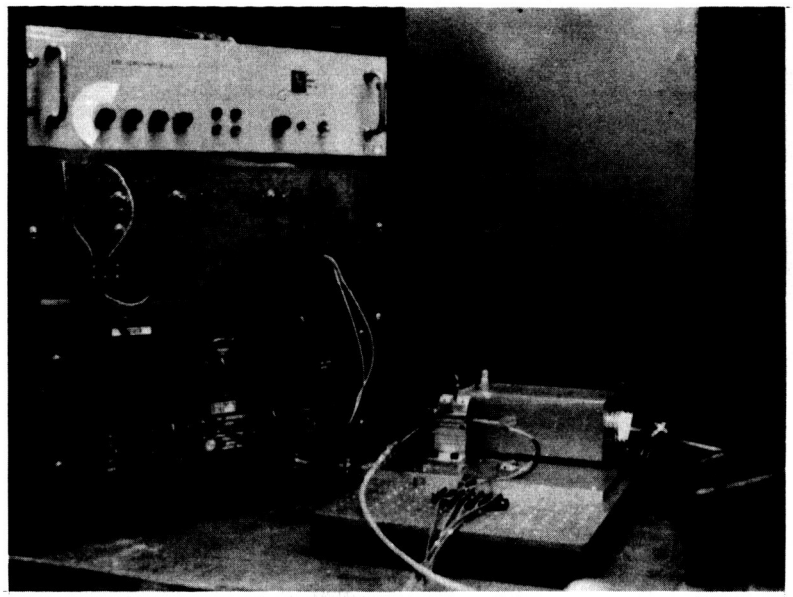

Fig. 4. Torque Motor, Flapper Valve, and Chamber of the Pneumatic Function Chamber.

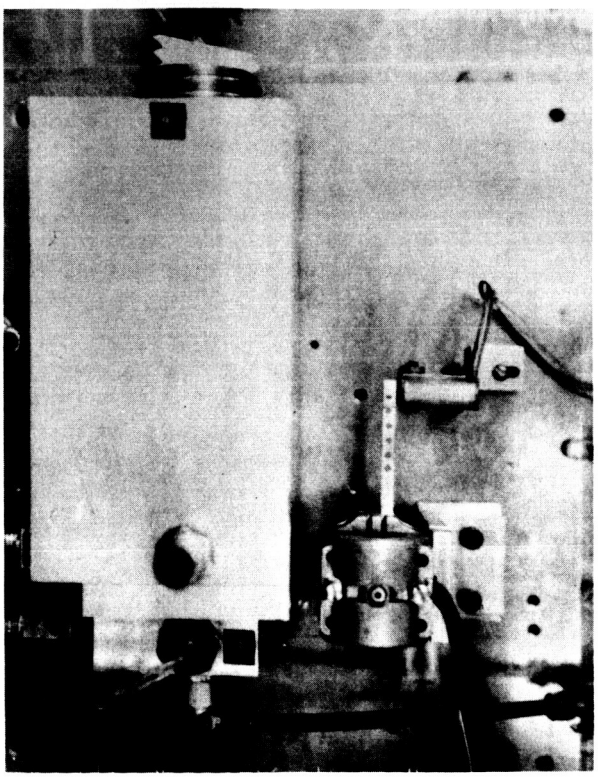

Fig. 5. Pneumatic Function Chamber.

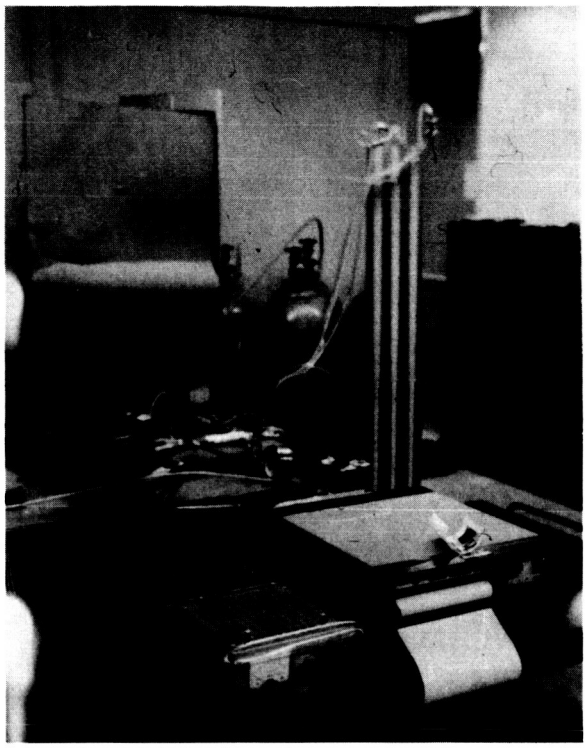

Fig. 6. HDL Proportional Amplifier Instrumented With Linear Flow Resistances and Pressure Transducers.

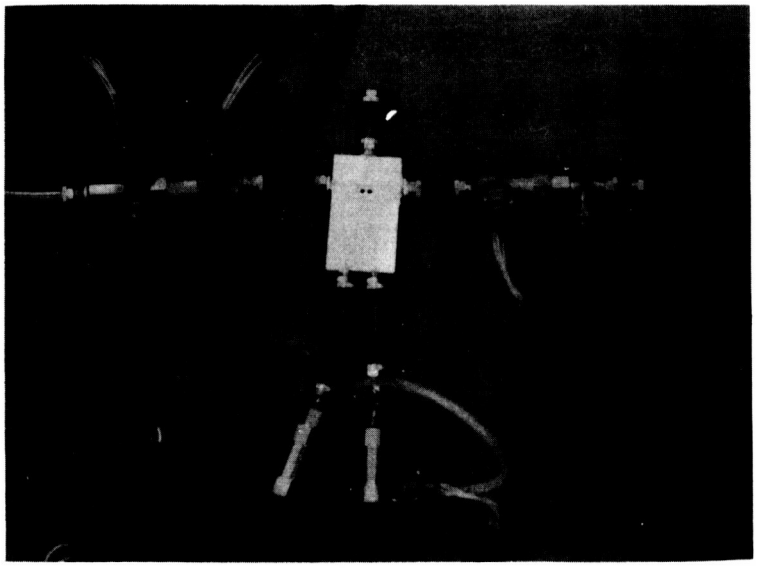

Fig. 7. Instrumentation System.

The control unit couples the transducers, power supply and recorder and also enables individual bridge balancing of the transducers. All external wiring is shielded and grounded. One of the six bridge balance circuits (which are connected in parallel) is represented in Fig. 8. In the background of Fig. 7 are the test element (HDL amplifier), flow regulators, air bottles, and pressure manometers.

The entire test setup is represented schematically in Fig. 9. The test procedure is actually quite simple:

1. Power on to torque motor (oscillator and amplifier), transducer supply, recorder.
2. Balance pressure transducers with control unit.
3. With air bottles closed, adjust constant pressure flows at test element ports. Open bottles and allow them to charge.
4. Flow on to wave generator. Adjust signal pressure.
5. Adjust recorder so that traces are conveniently spaced. Run recorder paper at desired speed.

The results of the experiment are five nearly sinusoidal traces, as shown in Fig. 10. Since the pressures at all ports except one are held constant, the four resulting admittance amplitude ratios and phase relations establish the four complex-number elements of the appropriate column of the admittance matrix:

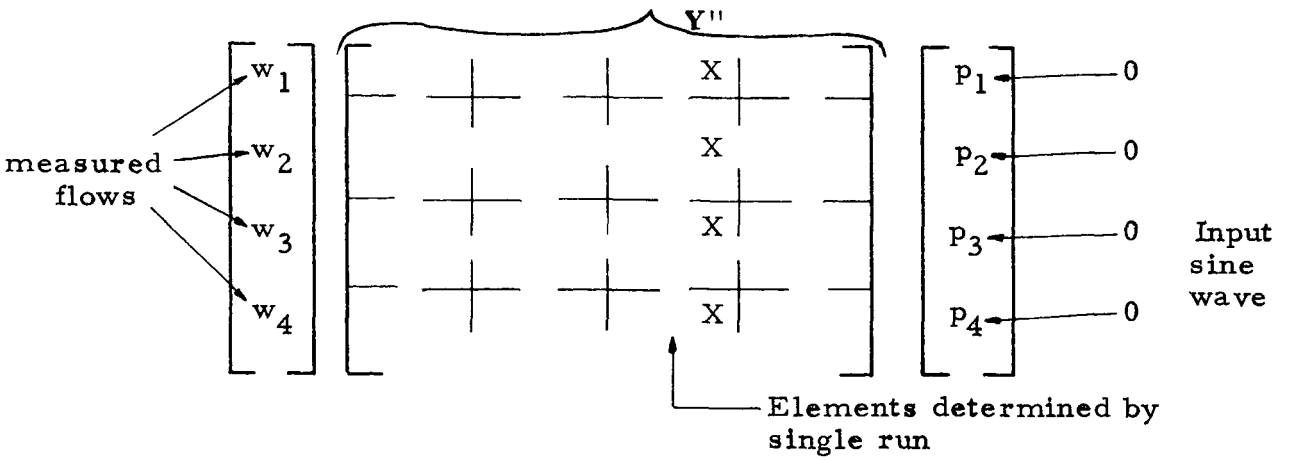

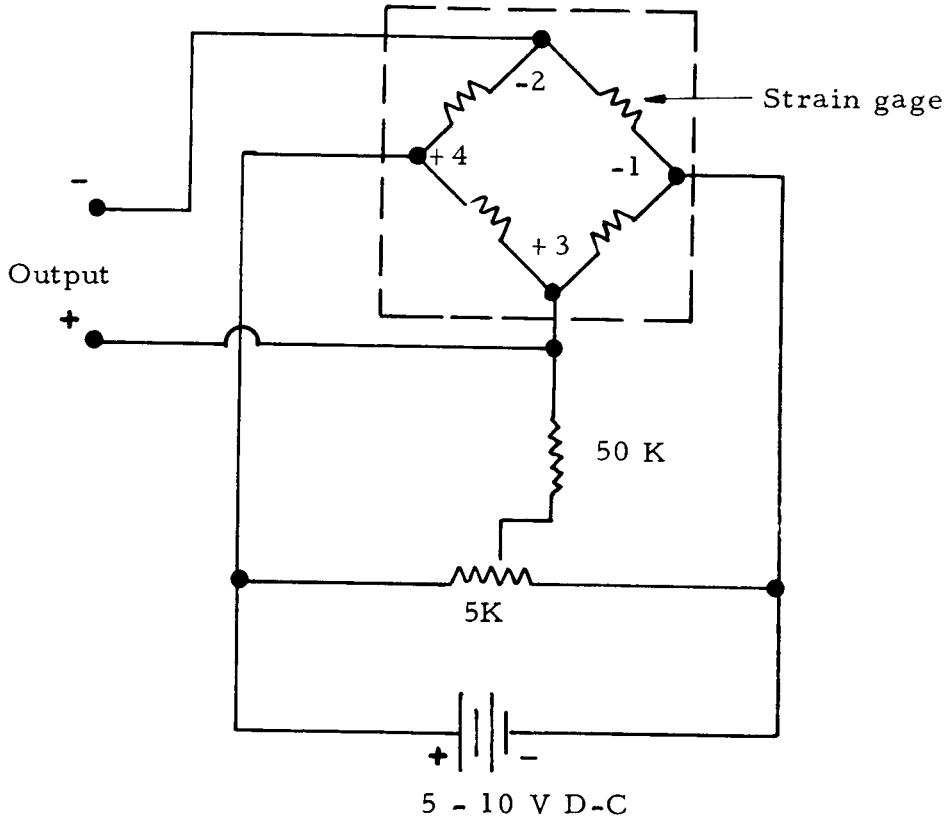

Fig. 8. Bridge Balance Circuit Diagram.

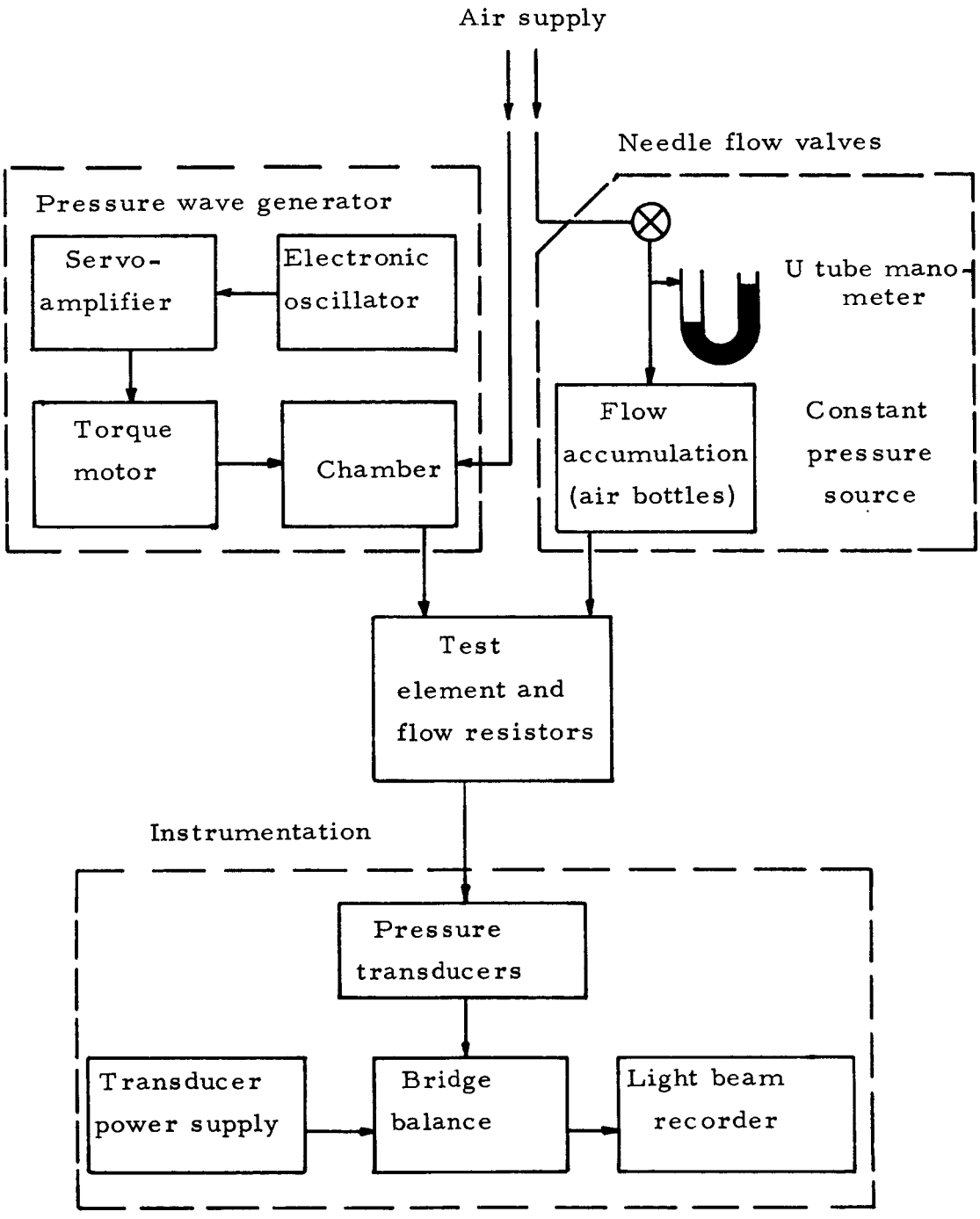

Fig. 9. Schematic of Test Arrangement.

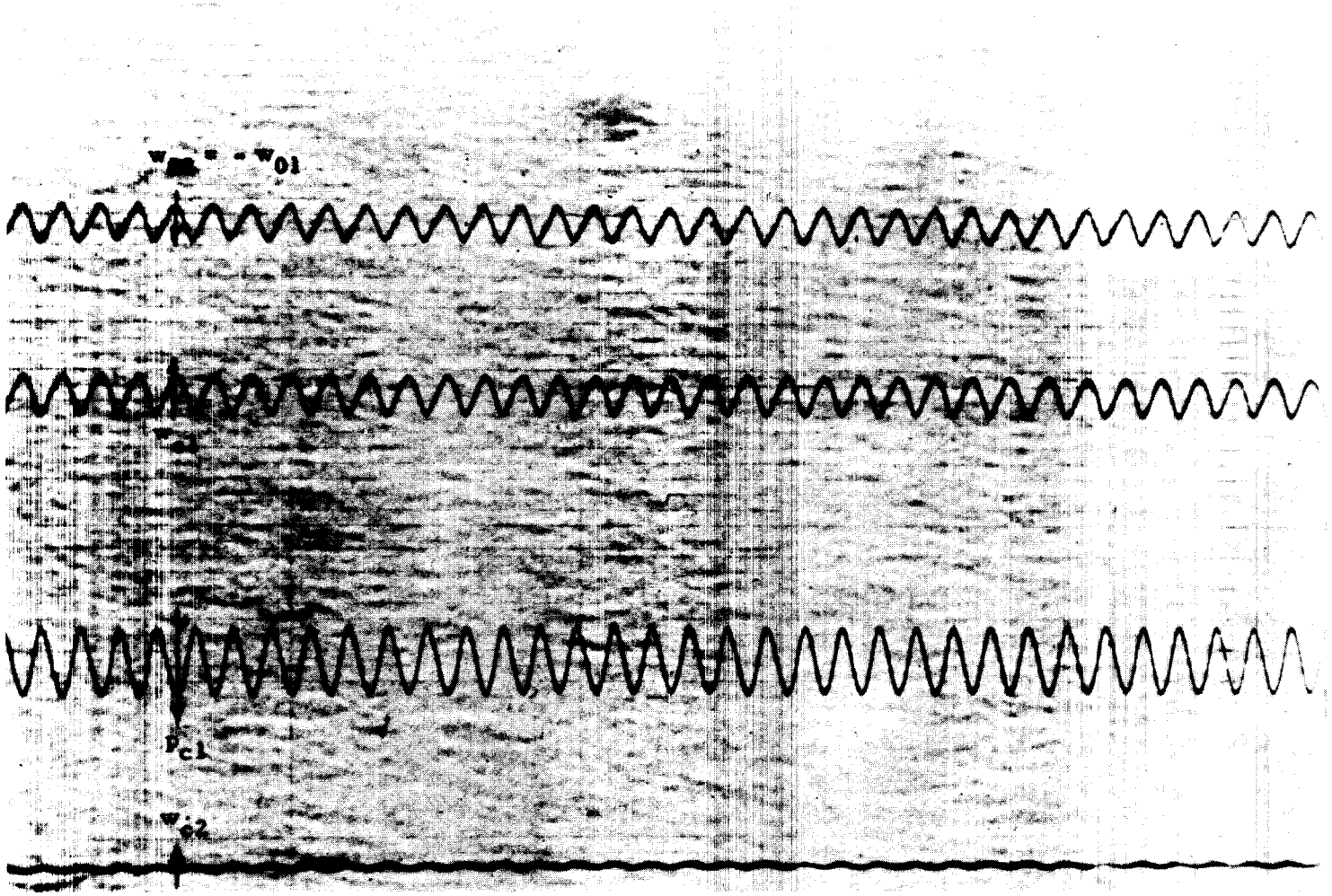

Fig. 10. Light Beam Recorder Traces Giving First Two Columns of Eq. 42. The Transducer Measuring the Output Flow, w_{02}, has 1/3 the Sensitivity of the Others. (Positive Flow is into the Element).

Three additional runs using the other inputs, and making certain the time average pressure at each port is the same for each run, establish the remainder of the matrix. Of course, a total of only two runs are necessary if the device and the average boundary pressures are symmetric.

The matrix $\mathbf{Y}''$ thus determined is for the amplifier plus the flow-measuring resistances at each port. We would like, rather, the matrix $\mathbf{Y}$ of the amplifier alone. To get this, $\mathbf{Y}''$ is inverted to get the impedance matrix $\mathbf{Z}''$, from which the peripheral resistances are easily stripped:

$$\mathbf{Y} = \left[(\mathbf{Y}'')^{-1} - \mathbf{R}\right]^{-1} \tag{41}$$

The resistance matrix $\mathbf{R}$ is diagonal, with each of the four non-zero elements equalling the resistance of the associated resistor.

The above procedure is illustrated in the following section.

If an amplifier or other element being tested is essentially linear, only one matrix $\mathbf{Y}$ is needed to describe its behavior at any given frequency. However, if it is nonlinear, other matrices are appropriately determined for different operating mean pressures. For stability considerations probably only the range of the matrix elements is necessary.

Below a certain frequency the dynamics of the amplifier is negligible and only one matrix $\mathbf{Y}$ with real elements need be found, aside from the effects of nonlinearities. It is probably impractical to use this whole procedure for very high frequencies when the dynamics of the physical resistor and its coupling become significant. Thus an alternative wave approach is outlined in Sec. 6.

5. EXPERIMENTAL RESULTS - HDL AMPLIFIER

The single-stage HDL-Corning amplifier, shown in Figs. 6 and 11, was tested at a low frequency (about 4 cps) for which the admittance matrix was real. This test is a forerunner of extensive tests of this and other amplifiers, and is included herein to demonstrate the use of the experimental-analytical procedure. The output pressures were adjusted until the output flows had a zero time average. The nozzle supply pressure was 10 inches Hg and the time-average pressure upstream of the control-flow metering resistors was 4 inches Hg. The admittance matrix required only two runs (one shown in Fig. 10) since the device and the boundary time-average pressures were symmetrical:

$$\begin{bmatrix} w_{c1} \\ w_{c2} \\ w_{01} \\ w_{02} \end{bmatrix} = \underbrace{\begin{bmatrix} 1.88 & 0.15 & 0 & 0 \\ 0.15 & 1.88 & 0 & 0 \\ 4.93 & 4.93 & 2.71 & 0.39 \\ -4.93 & 4.93 & 0.39 & 2.71 \end{bmatrix}}_{\mathbf{Y}'' \text{ all units cfh/psi}} \begin{bmatrix} p_{c1} \\ p_{c2} \\ p_{01} \\ p_{02} \end{bmatrix} \qquad (42)$$

The sign of the output transfer admittance (value 0.39) came as a surprise, incidentally. The flow-measuring resistors had previously been tested, and found to be linear but with a uniformly higher resistance than that reported by the manufacturer:

$$\mathbf{R} = \begin{bmatrix} 0.312 & 0 & 0 & 0 \\ 0 & 0.312 & 0 & 0 \\ 0 & 0 & 0.312 & 0 \\ 0 & 0 & 0 & 0.312 \end{bmatrix} \quad \text{All units psi/cfh} \qquad (43)$$

Consequently, from Eq. (41) and after some arithmetric,

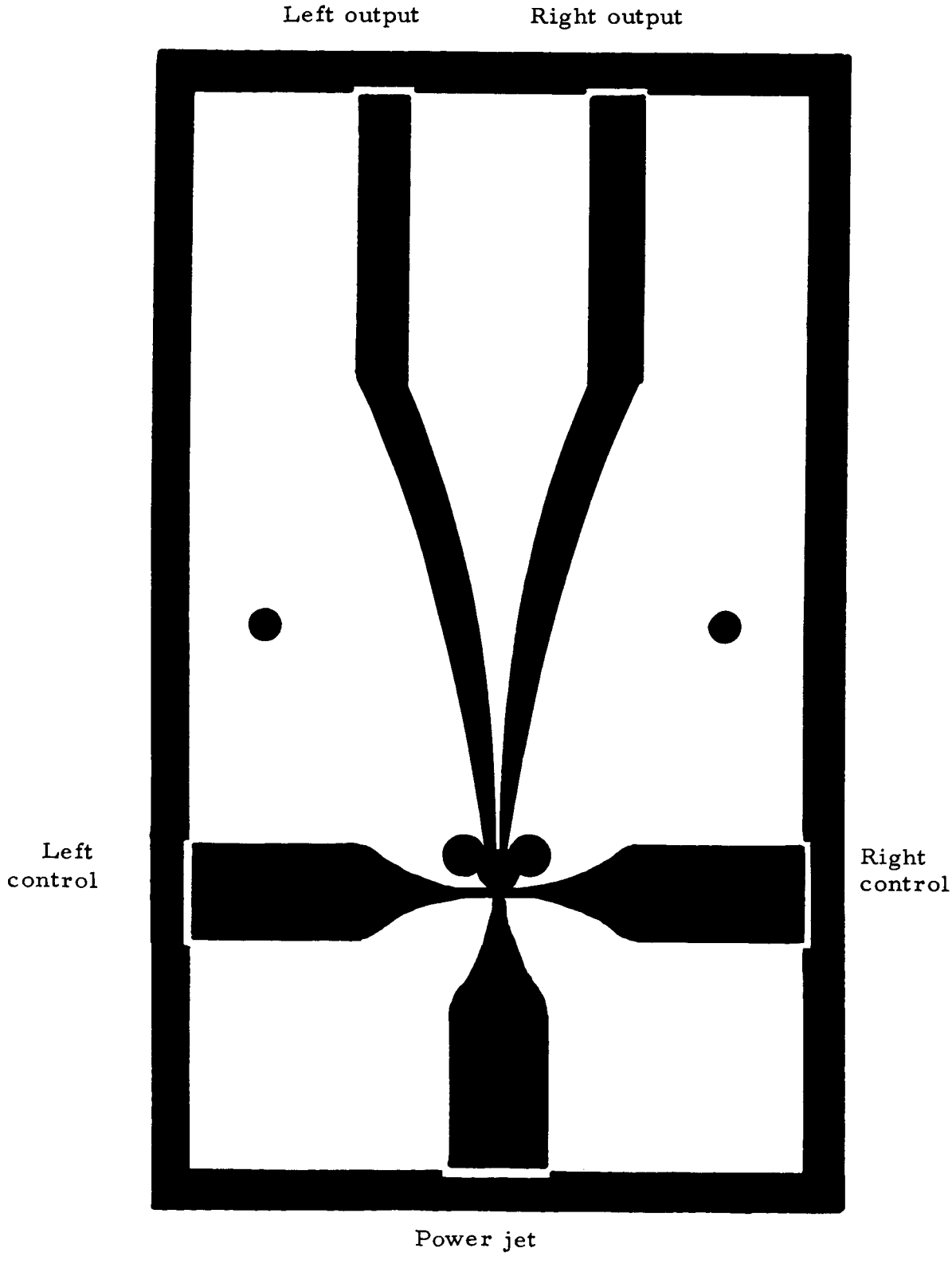

Fig. 11. HDL-Corning Single Stage Proportional Amplifier.

$$\mathbf{Y} = \begin{bmatrix} 4.65 & 0.89 & 0 & 0 \\ 0.89 & 4.65 & 0 & 0 \\ 38.8 & -38.8 & 51.5 & 43.1 \\ -38.8 & 38.8 & 43.1 & 51.5 \end{bmatrix} \quad \begin{matrix} \text{All units} \\ \text{cfh/psi} \end{matrix} \qquad (44)$$

Let us use this result to predict the stability or lack of stability for two very simple but common systems, and then check the predictions with actual experience. First, we might expect an instability if the two output ports are connected together with a moderately long line. For this purpose we can neglect all except the lower-right quadrant of the matrix, since p_{c1} and p_{c2} will be held essentially constant (which means zero in terms of our approach because only the A-C components are under consideration). Actually the true values of these admittances may be some what different under these conditions, but only very slight sensitivity is expected to the mean control pressure. Therefore we substitute

$$\begin{aligned} Y_{11} &= 51.5 \\ Y_{12} &= 43.1 \end{aligned} \qquad (45)$$

into Eq. (30) and find the system should be markedly stable. Experiment corroborated this result.

Our second example involves connecting one output port to the control port on the same side with a moderately long line. Again only four elements of the 16-element admittance matrix need be used, since the other ports had constant pressures.

$$\begin{bmatrix} w_{c1} \\ w_{01} \end{bmatrix} = \begin{bmatrix} Y_{11} & Y_{12} \\ Y_{21} & Y_{22} \end{bmatrix} \begin{bmatrix} p_{c1} \\ p_{01} \end{bmatrix} = \begin{bmatrix} 4.65 & 0 \\ 38.8 & 51.5 \end{bmatrix} \begin{bmatrix} p_{c1} \\ p_{01} \end{bmatrix} \qquad (46)$$

This time, however, the system is asymmetric and consequently Eq. (34) and its complement (reversed subscripts) are utilized. Since $Y_{12} = 0$, the criterion for stability reduces to

$$Y_{22}^2 Y_{11} Z_c^2 + 2(Y_{22} Y_{11} - Y_{21}^2) Z_c + Y_{11} > 0 \tag{47}$$

or

$$12,314 Z_c^2 - 1,457 Z_c + 4.65 > 0 \tag{48}$$

which is true for large Z_c and small Z_c. But for intermediate Z_c

$$0.0033 < Z_c < 0.1151 \text{ psi/cfh} \tag{49}$$

A 1/4 inch I.D. tube was used, for which

$$Z_c = \frac{\rho c_o}{\pi a^2} = \frac{kp}{\pi a^2 c_o} = \frac{1.4 \times 14.7 \times 144}{\pi(0.25)^2 \times 1100 \times 3600} = 0.00619 \text{ psi/cfh} \tag{50}$$

and, indeed, the system was unstable when tested. It produced an audible tone at the half-wave length frequency (about 100 cps), as was expected.

Thus data taken at 4 cps was useful at 25 times that frequency. We intend to investigate the useful range over which static data can be applied.

6. HIGH FREQUENCY OR WAVE APPROACH

An experimental approach toward directly measuring the elements of the wave-scattering matrix (see Sec. 2.2) has been proposed by one of the authors[+]. M.I.T. doctoral candidate, L. E. Johnston, under the supervision of this author, has been pursuing an unsponsored investigation, using these techniques, into the dynamics of a fluid jet incident on two receiver ports. His experience will help guide R. E. Wallhagen, who very recently joined the present contract effort as a Research Assistant specifically to utilize wave techniques to determine the high-frequency characteristics of fluid jet amplifiers and associated components.

The travelling-wave line of the apparatus described in the above-mentioned paper must have a perfect reflectionless termination, or an undesired standing-wave pattern will appear. L. E. Johnston is concerned with very high frequencies, up to and above 10 KC, and consequently abandoned the concept of a passive termination. It would be very difficult to design a passive termination which, at these frequencies, would have the necessary purely resistive (no inductance) characteristic.

In the scope of the present effort, however, frequencies of greatest interest probably will be below 2 KC. Thus R. E. Wallhagen is preparing to test dynamically, with incident and reflected waves, a porous filter disk made by Mott Metallurgical Corporation. Wallhagen's measurements of the static characteristics of the 1/16 inch thick disk, mounted with an exposed circular area of 1/2 inch diameter, are shown in Fig. 12. Also shown is the characteristic which would ideally match a 1/2 inch line; apparently only a small area change is necessary to compensate for the difference. However, the frequency above which the impedance characteristic is significantly different due to inductance, etc., is not known.

Johnston's approach, which will be adopted if necessary, involves an active termination, consisting of a hi-fi driver much like the original wave generator. The scheme is shown in Figs. 13 and 14. Reflections are eliminated by careful adjustment of the phase shifter and associated amplifiers. The absence of standing waves is observed from the response of two pressure transducers mounted one-half on one-quarter wave length apart.

[+] ibid

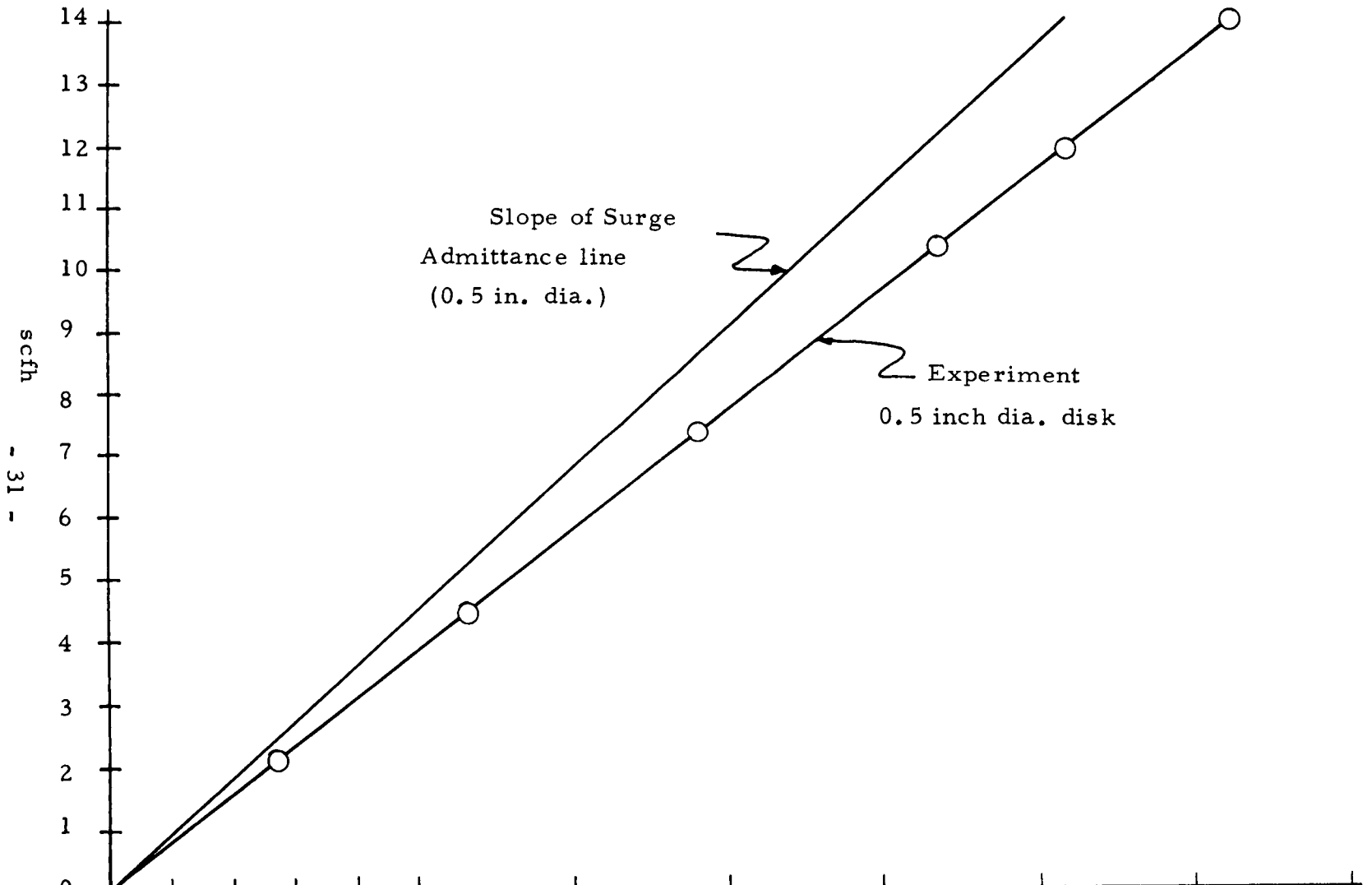

Fig. 12. Corrected Resistance Relation of Mott Porous Disk.

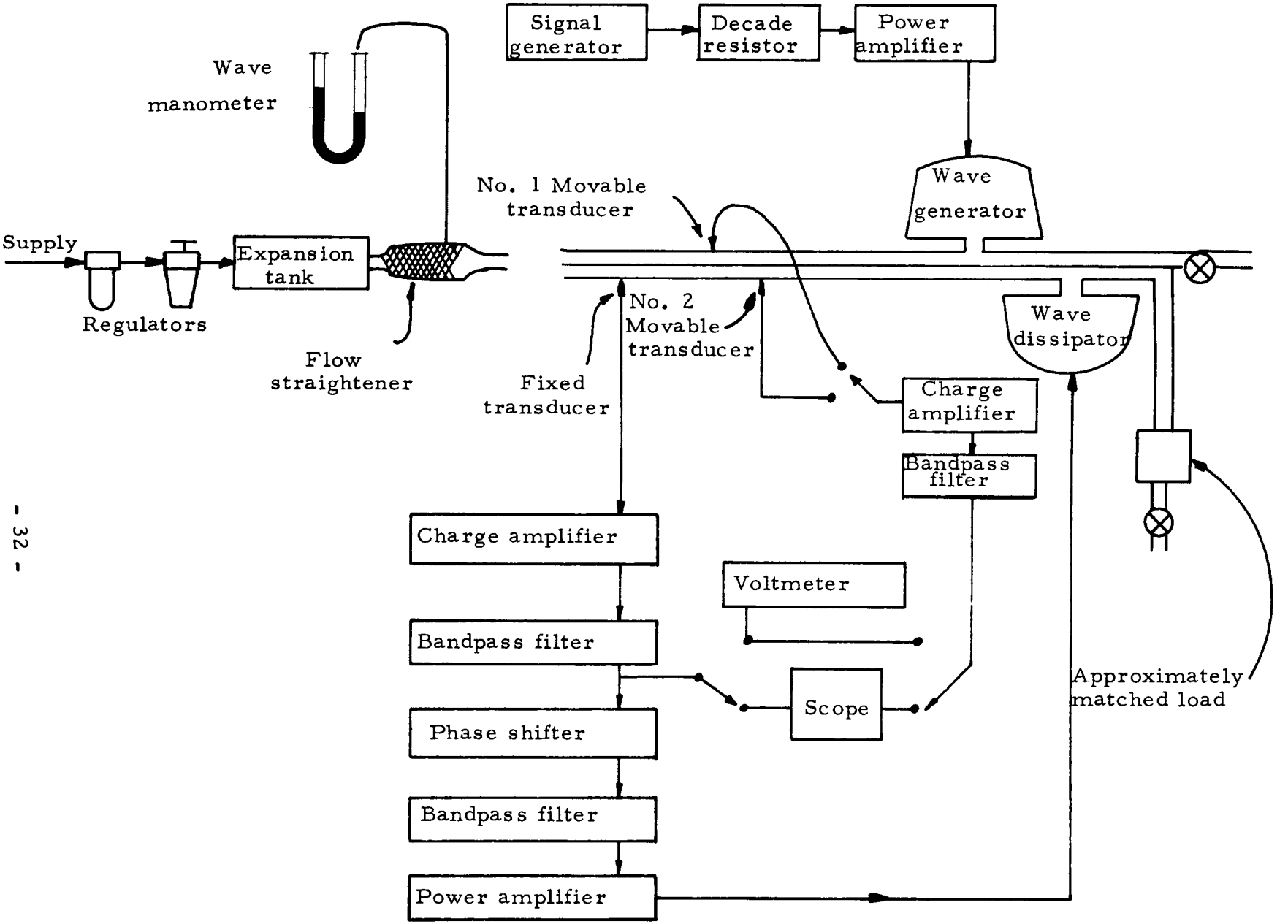

Fig. 13. Experimental Apparatus of L. E. Johnston.

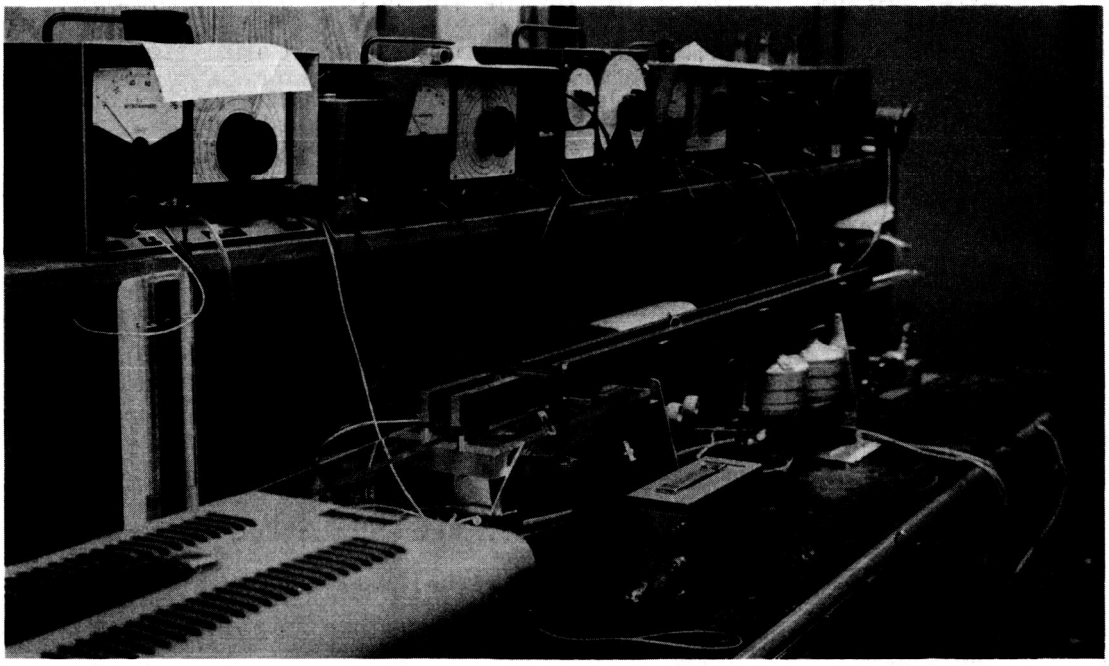

a. Over-all View

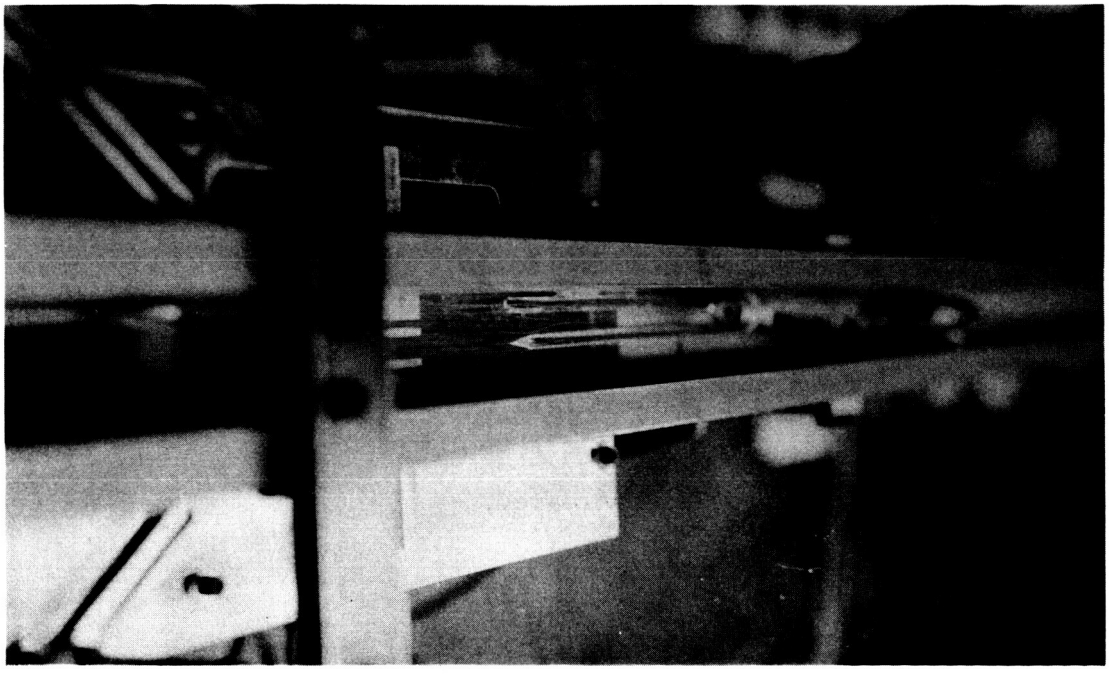

b. Jet Interaction Region

Fig. 14. Photographs of Johnston's Apparatus.

The effect of wave attenuation on the shape of the standing-wave pattern in the standing-wave line has been investigated analytically by Johnston. The ratio of the total shift between an adjacent node and antinode, due to wall shear induced attenuation, to the lossless node-antinode spacing is

$$R = \frac{2}{\pi} \sin^{-1}\left[\frac{a\lambda(1 - r^2)}{4\pi r}\right] \tag{51}$$

where λ is the nominal wavelength, a the attenuation factor (single waves attenuate along the line as $\exp(-ax)$, where x is the position), and r the magnitude of the reflection coefficient at the end of the line. In practice this ratio is almost negligibly small unless r is very small (usually $r > 0.5$) or the attenuation per wavelength extraordinarily great. If r is very small, however, the significances of the result is fortunately also very small; it vanishes when $r = 0$.

The effect of wall friction on the node and antinode amplitudes is significant. For the transducer locations of Fig. 15, the magnitude of the reflection coefficient is

$$r = \frac{p_{an} e^{\frac{a\lambda}{4}} - p_n}{p_{an} e^{\frac{a\lambda}{4}} + p_n} e^{2aL} \tag{52}$$

when

$$r < e^{2a(L - \frac{\lambda}{4})} \tag{53}$$

when the inequality of Eq. (53) is violated,

$$r = \frac{p_{an} e^{-\frac{a\lambda}{4}} + p_n}{p_{an} e^{\frac{a\lambda}{4}} - p_n} e^{2aL} \tag{54}$$

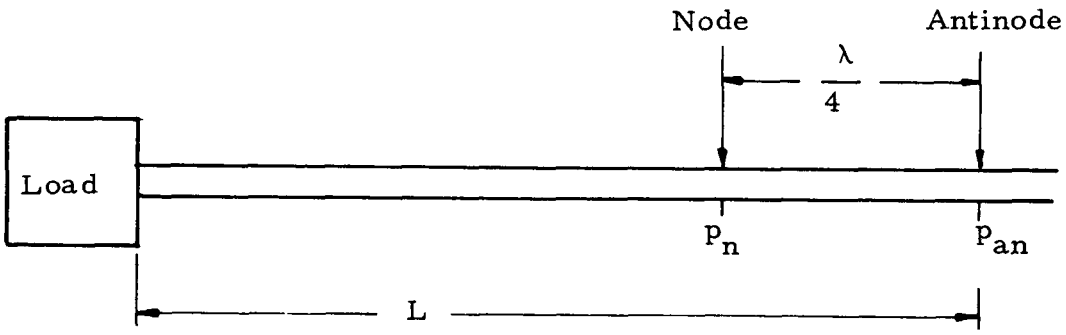

Fig. 15. Measurements to Determine Reflection Coefficient.

The phase of the reflection coefficient can be determined from the locations of the node and antinode.

To experimentally determine the value of α the oscillation amplitudes of two adjacent nodes, p_1 and p_3, and the mid-way antinode, p_2, can be used in the following equation:

$$\frac{p_1 - p_3}{p_2} = \frac{1 - e^{-\alpha\lambda}}{e^{\frac{-3\alpha\lambda}{4}} + e^{\frac{\alpha\lambda}{4}}} \tag{55}$$

The relationship is virtually linear up to about $\alpha\lambda = 0.4$, and deviates from linearity by only 1 per cent at $\alpha\lambda = 1.0$.

It must be remembered that, except at very high frequencies, the phase velocity of waves in a tube is less than in unconfined space.[+]

[+] Brown, F.T., "The Transient Response of Fluid Lines", ASME Transactions, Journal of Basic Engr., December 1962.

DISTRIBUTION LIST

NASA-Lewis Research Center (3)
21000 Brookpark Road
Cleveland, Ohio 44135
Attention: W. S. Griffin, MS 54-1

NASA-Lewis Research Center (2)
21000 Brookpark Road
Cleveland, Ohio 44135
Attention: Lewis Library

NASA-Lewis Research Center (1)
21000 Brookpark Road
Cleveland, Ohio 44135
Attention: James E. Burnett,
Technology Utilization
Office

NASA-Ames Research Center (1)
Moffett Field, California 94035
Attention: Library

NASA-Goddard Space Flight Center (1)
Greenbelt, Maryland 20771
Attention: Library

NASA-Marshall Space Flight Center (1)
Huntsville, Alabama 35812
Attention: Library

NASA-Marshall Space Flight Center (1)
Huntsville, Alabama 35812
Attention: Michael A. Kalange,
R-ASTR-NF

NASA-Western Operations (1)
150 Pico Boulevard
Santa Monica, California 90406

NASA Scientific and Technical
Information Facility (6)
Box 5700
Bethesda, Maryland
Attention: NASA Representative

NASA-Lewis Research Center (1)
21000 Brookpark Road
Cleveland, Ohio 44135
Attention: John Danicic, MS 54-1

NASA-Lewis Research Center (1)
21000 Brookpark Road
Cleveland, Ohio 44135
Attention: Lewis Technical Information
Division

NASA Headquarters (1)
Washington, D. C. 20546
Attention: F. C. Schwenk, NPO

NASA-Flight Research Center (1)
P. O. Box 273
Edwards, California 93523
Attention: Library

NASA-Langley Research Center (1)
Langley Station
Hampton, Virginia 23365
Attention: Library

NASA-Marshall Space Flight Center (1)
Huntsville, Alabama 35812
Attention: Roy E. Currie, Jr.; R-ASTR-TN

NASA-Manned Spacecraft Center (1)
Houston, Texas 77001
Attention: Library

Jet Propulsion Laboratory (1)
4800 Oak Grove Drive
Pasadena, California 91103
Attention: Library

Harry Diamond Laboratories (3)
Washington 25, D. C.
Attention: Joseph M. Kirshner

Harry Diamond Laboratories (2)
Washington 25, D. C.
Attention: Library

Wright-Patterson Air Force Base (2)
Ohio
Attention: Library

U. S. Atomic Energy Commission (1)
Technical Information Service Extension
P. O. Box 62
Oak Ridge, Tennessee

NASA-Langley Research Center (2)
Langley Station
Hampton, Virginia 23365
Attention: Mr. David Garner

NASA Headquarters, Code REI (1)
Office of Advanced Research & Technology
Washington, D. C. 20425
Attention: Mr. Stuart Vogt

USAF Avionics Laboratory (2)
Wright Patterson AFB, Ohio 45433
Attention: Mr. Seth Young (AVNE)

NASA Electronics Research Laboratory (1)
545 Technology Square
Cambridge, Massachusetts 02139
Attention: Dr. George Kovatch

NASA Headquarters (1)
Washington, D. C. 20546
Attention: Mr. John Morrissey, NPO

Army Missile Command (2)
Redstone Arsenal
Huntsville, Alabama
Attention: Library

U. S. Atomic Energy Commission (2)
Technical Reports Library
Washington, D. C.

Los Alamos Scientific Laboratory (1)
Los Alamos, New Mexico
Attention: Joseph Perry, N-4

NASA-Lewis Research Center (2)
21000 Brookpark Road
Cleveland, Ohio 44135
Attention: Nuclear Rocket Technology
Office

USAF Flight Dynamics Laboratory (1)
Wright Patterson AFB, Ohio 45433
Attention: Mr. James Hall (FDCL)

Army Missile Command
Redstone Arsenal
Huntsville, Alabama
Attention: Mr. Thomas Wetheral

Air Force Weapons Laboratory (1)
Kirtland AFB, New Mexico
Attention: Capt. Charles W. Fada (WLDC-1)

Case Institute of Technology (2)
Mechanical Engineering Department
Cleveland, Ohio
Attention: Dr. Charles Taft